Title

COMPARISON OF BACKSCATTERING INTENSITIES FOR LOW ENERGY ELECTRONS FROM VARIOUS SURFACE ATOMS (H, Li, Be, C, O, Al, Si, S, V, Cr, Ni, Cu, Ag, Pt. Au)

Authors

Fink, M.
Martin, M.R.
Somorjai, G.A.

Publication Date

1971-08-01

Submitted to Surface Science

COMPARISON OF BACKSCATTERING INTENSITIES FOR LOW ENERGY ELECTRONS FROM VARIOUS SURFACE ATOMS (H, Li, Be, C, O, Al, Si, S, V, Cr, Ni, Cu, Ag, Pt, Au)

M. Fink, M. R. Martin, and G. A. Somorjai

August 1971

AEC Contract No. W-7405-eng-48

LAWRENCE RADIATION LABORATORY
UNIVERSITY of CALIFORNIA BERKELEY

DISCLAIMER

COMPARISON OF BACKSCATTERING INTENSITIES FOR LOW ENERGY ELECTRONS FROM VARIOUS SURFACE ATOMS (H, Li, Be, C, O, Al, Si, S, V, Cr, Ni, Cu, Ag, Pt, Au)

M. Fink

Electronics Research Center and Department of Physics
The University of Texas at Austin

and

M. R. Martin* and G. A. Somorjai

Departments of Chemistry and Physics of the University of California
at Berkeley and Inorganic Materials Research Division
Lawrence Berkeley Laboratory, Berkeley, California 94720

ABSTRACT

The atomic scattering factors for various elements are compared in the energy range (50-180 eV) employed in low energy electron diffraction (LEED) studies at backscattering angles in order to obtain estimates of their relative strengths. The scattered intensity from atomic hydrogen is about two orders of magnitude smaller than that from metals commonly used as substrates in surface studies by LEED. Carbon and oxygen have scattered intensities of the same order of magnitude as many metals at 50 eV but these intensities decrease monatomically as the incident electron energy is increased.

*Work supported in part by National Science Foundation Grant No. GP 13889.

The power of Low Energy Electron Diffraction (LEED) techniques to probe the periodic surface structures of crystals and adsorbed layers has not yet been fully realized. Although the literature contains much reliable experimental data[1] on the properties of the diffraction beams as a function of energy and scattering angle from a number of solid surfaces and various adsorbates, the theoretical complexity of the multiple scattering problem has until recently prohibited direct interpretation of these results. Recently, however, encouraging progress has been reported in matching theoretically calculated beam intensity profiles as a function of incident electron energy to the experimental data.[2] It thus seems likely that the LEED technique will soon enable the experimentalist to obtain detailed three dimensional structural information at crystal surfaces.

The theoretical complexities in the interpretation of LEED patterns are a direct consequence of the scattering properties of low energy (30 → 500 eV) electrons that also make them potentially valuable for surface analysis; namely, the large atomic collision cross sections in this energy range. It is the large elastic cross section (together with inelastic damping processes) which limits penetration of such electrons to several crystal layers, making them suitable probes for surface structure. On the other hand, the large cross sections make multiple scattering processes highly probable, requiring a more complex theoretical analysis than for the kinematic theories that have been successful in the intrepation of X-ray and neutron diffraction work. Furthermore, a description of the electron scattering process in this energy range is complicated by the breakdown of the Born approximation. The use of isolated atomic

scattering factors $f(\theta,E)$ for low energy elastic electron scattering can be justified as a good approximation to the true electron-crystal scattering mechanism.[3] A large momentum transfer must be imparted to an electron in this energy range in order to cause it to be reflected through a sufficient angle ($\theta > 140°$) to be detected by the LEED apparatus. Such electrons must penetrate deeply into the strong atomic potential fields near the nucleus in order to undergo backscattering,[4] whereas typical solid state effects are due to the redistribution of electrons from the outermost atomic shells.

It is the purpose of this paper to report on some recent atomic scattering factor calculations in a manner that will make them useful as a guide to LEED experimentalists. Although multiple scattering is of great importance in the detailed analysis of experimental results, single scattering processes are always present, and in some cases appear to be dominant.[5] The intensity of the backscattered low energy electron beams depends on the scattering factor $f(\theta,E)$ of the atom embedded in the surface, and the crystal structure factor. These two factors are separable only in the case of single scattering processes. Nevertheless, it is useful to compare the atomic scattering factors for various elements at backscattering angles in the energy range employed by LEED studies in order to obtain an order of magnitude estimate of their relative strengths. Such considerations are especially important to the researcher who desires to investigate the structure of an adsorbed layer (oxide, hydrocarbon layer, etc.) on a solid single crystal substrate. Comparison of the scattering intensities $|f(\theta,E)|^2$ of the atoms present in the adsorbed layer with those in the substrate will give an indication of the sensitivity

of the LEED experiment to the surface structure throughout the energy range of interest. It will be noted, from Figs. 1, 2 and 3, that the electron scattering intensity from atomic hydrogen is about two orders of magnitude less than that from the metals commonly used as substrates. One would therefore not expect to readily observe surface structure due to hydrogen against the relatively intense background from a metallic surface. This result strongly supports the model of substrate reconstruction[6] under conditions where hydrogen adsorption produces the appearance of fractional order diffraction beam intensities that are comparable to the beam intensities from the clean metallic surface.

It is also of interest to point out that carbon and oxygen, both important elements in the study of adsorbed layers, have scattering intensities of the same order of magnitude as many metals near 50 eV, but that these intensities decrease monotonically as the incident electron energy is increased, whereas the scattering intensities of metals do not show such a simple energy dependence. From such considerations, it appears feasible to distinguish between scattering from oxygen and metal atoms by analysis of the energy dependence of the scattered intensity.

Atomic scattering factors have been calculated for a number of elements using a computer program developed by A. C. Yates.[7] This program is based on the numerical solution of the Dirac equation by partial wave analysis, and the computation is terminated automatically when the scattering amplitudes reach stability to five significant figures. The reliability of the calculated results is limited by the atomic potentials employed, as well as by second order effects like charge cloud polarization and exchange contributions between the incident and atomic electrons.[8]

The atomic potentials are derived from relativistic Hartree-Fock-Slater wavefunctions and are extremely accurate. Comparison of this potential with a relativistic Hartree-Fock potential for Hg showed very good agreement in the scattering factors.[9] It has been shown experimentally and theoretically that charge cloud polarization has a negligible effect on the scattering factors at angles in excess of 30° for all atoms.[10] The inclusion of exchange between the incident and atomic electrons for very heavy atoms alters the scattering factors by about 20%, but these deviations should decrease rapidly for smaller Z-values. In the angular regions near minima of the differential cross section the percentage deviation can be as large as 100% for low incident electron energies.[11]

In most of the calculations carried out at $\theta = 180°$, phase shifts up to $\ell = 10$ have been included. In a number of cases these were compared to calculations in which ℓ was allowed to reach a maximum value of 50 before the computation was terminated. In most cases the two values for the scattering intensity agreed to within 10% over the energy range investigated. This is encouraging since the necessity to include large ℓ-values to adequately describe the electron-atom scattering process in solids rapidly makes a computer program unwieldy and time consuming when calculating LEED intensities. Indeed, in many cases the inclusion of phase shifts corresponding to four or five ℓ-values should suffice, especially in the lower region of the LEED energy range.

Acknowledgments

The authors gratefully acknowledge many helpful discussions with Professor L. M. Falicov. This work was done under the auspices of the U. S. Atomic Energy Commission.

References

1. F. Jona, IBM Journal of Research & Development 14, no. 4, 444 (1970).
   H. H. Farrell, Ph. D. thesis, University of California, Berkeley, UCRL-19087, 1969.
   J. M. Baker, Ph. D. thesis, Cornell University (1970).
   R. M. Goodman, H. H. Farrell, and G. A. Somorjai, J. Chem. Phys. 49, 692 (1968).
   H. H. Farrell and G. A. Somorjai, Phys. Rev. 182, 751 (1969).
2. S. Y. Tong and T. N. Rhodin, Phys. Rev. Letters 26, 711 (1971).
   D. W. Jepsen, P. M. Marcus, and F. P. Jona, Fifth Low-Energy Electron Diffraction Seminar, March 1971.
   G. E. Laramore and C. B. Duke and A. Bagchi and A. B. Kunz (to be published).
3. M. R. Martin, G. A. Somorjai and M. Fink (to be published).
4. J. S. Schilling and Maurice B. Webb, Phys. Rev. B 2, 1665 (1970).
5. R. Kaplan and G. A. Somorjai, Solid State Comm. 9, 505 (1971).
   H. Tokutaka and M. Prutton, Surface Science 11, 216 (1968).
6. P. J. Estrup and J. Anderson, J. Chem. Phys. 45, 2254 (1966).
7. A. C. Yates, Computer Phys. Com. (accepted for publication).
8. M. Fink and A. C. Yates, Atomic Data 1, 385 (1970).
9. P. Moore and M. Fink, Phys. Rev. (accepted for publication).
10. R. A. Bonham, Phys. Rev. A3, 298 (1971).
11. D. W. Walker, J. Phys. B2, 356 (1969).

Figure Captions

Fig. 1. Logarithmic plot of scattering intensities $|f(\theta,E)|^2$ ($\AA^2$) for various atoms at a backscattering angle of $\theta = 180°$. Eleven phase shifts ($\ell = 0, 1, \cdots 10$) are employed in the calculation.

Fig. 2. Logarithmic plot of scattering intensities $|f(\theta,E)|^2$ ($\AA^2$) for various atoms at a backscattering angle of $\theta = 158°$. Eleven phase shifts ($\ell = 0, 1, \cdots 10$) are employed in the calculation.

Fig. 3. Logarithmic plot of scattering intensities $|f(\theta,E)|^2$ ($\AA^2$) for various atoms at a backscattering angle of $\theta = 158°$. Stability of $f(\theta,E)$ values is obtained to five significant figures by calculating phase shifts for up to 50 ℓ-values.

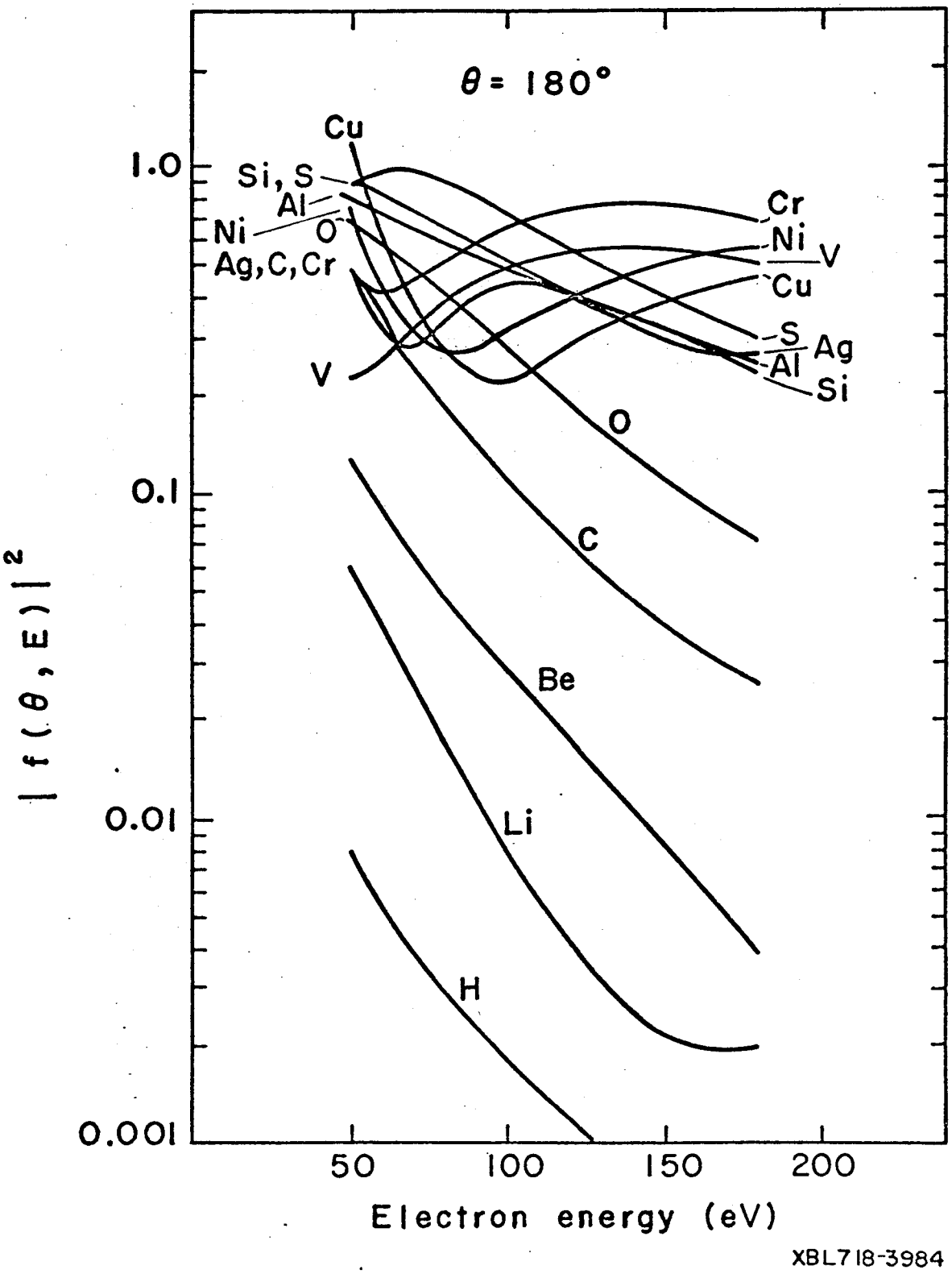
θ = 180°
Cu
Si, S
Al
Ni
O
Ag, C, Cr
V
Cr
Ni
V
Cu
S
Ag
Al
Si
O
C
Be
Li
H
1.0
0.1
0.01
0.001
50
100
150
200
Electron energy (eV)
|f(θ, E)|²
XBL718-3984

Fig. 1

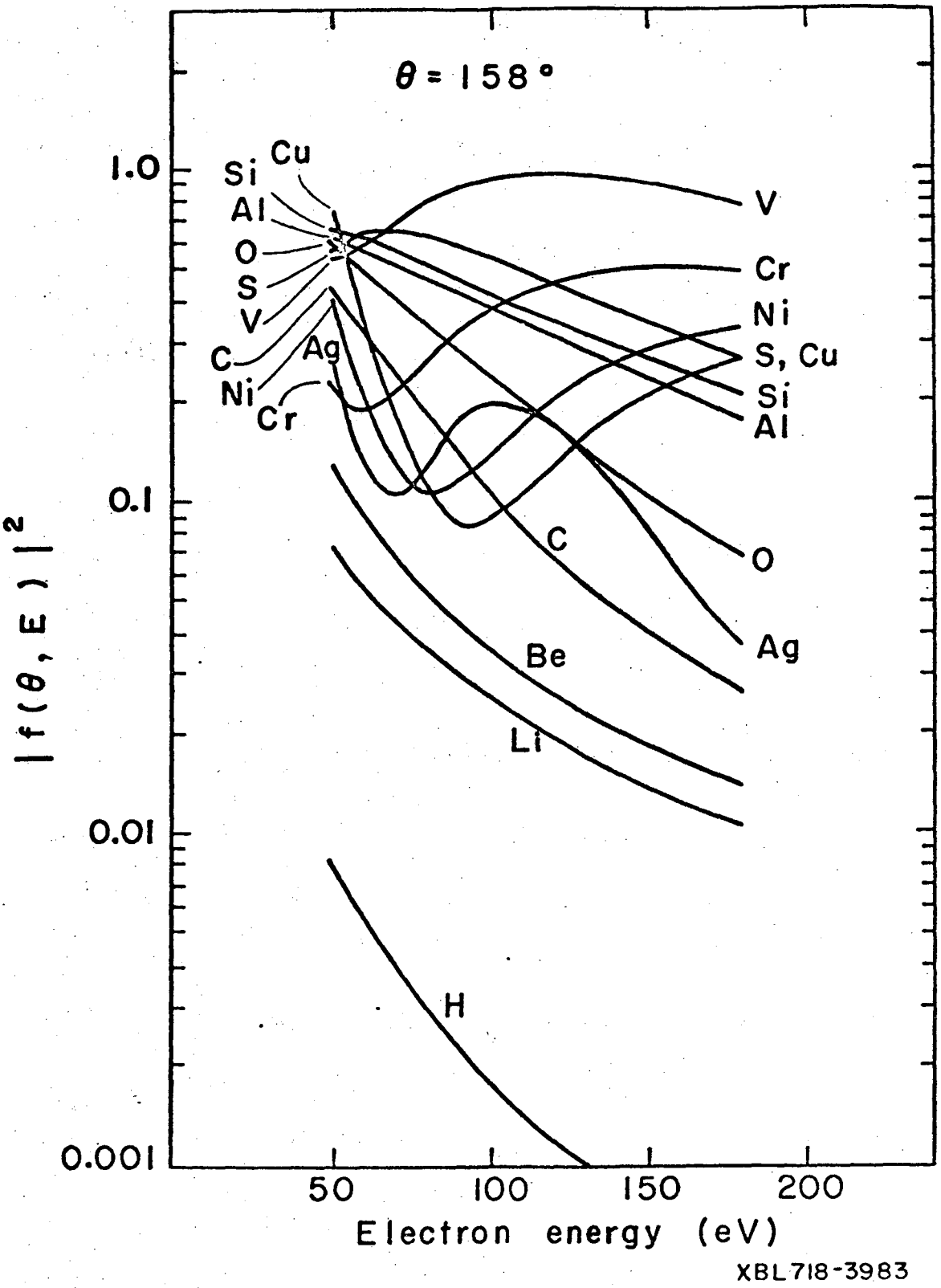
θ = 158°
1.0
0.1
0.01
0.001
$|f(\theta, E)|^2$
Si
Cu
Al
O
S
V
C
Ag
Ni
Cr
V
Cr
Ni
S, Cu
Si
Al
C
O
Ag
Be
Li
H
50
100
150
200
Electron energy (eV)
XBL718-3983

Fig. 2

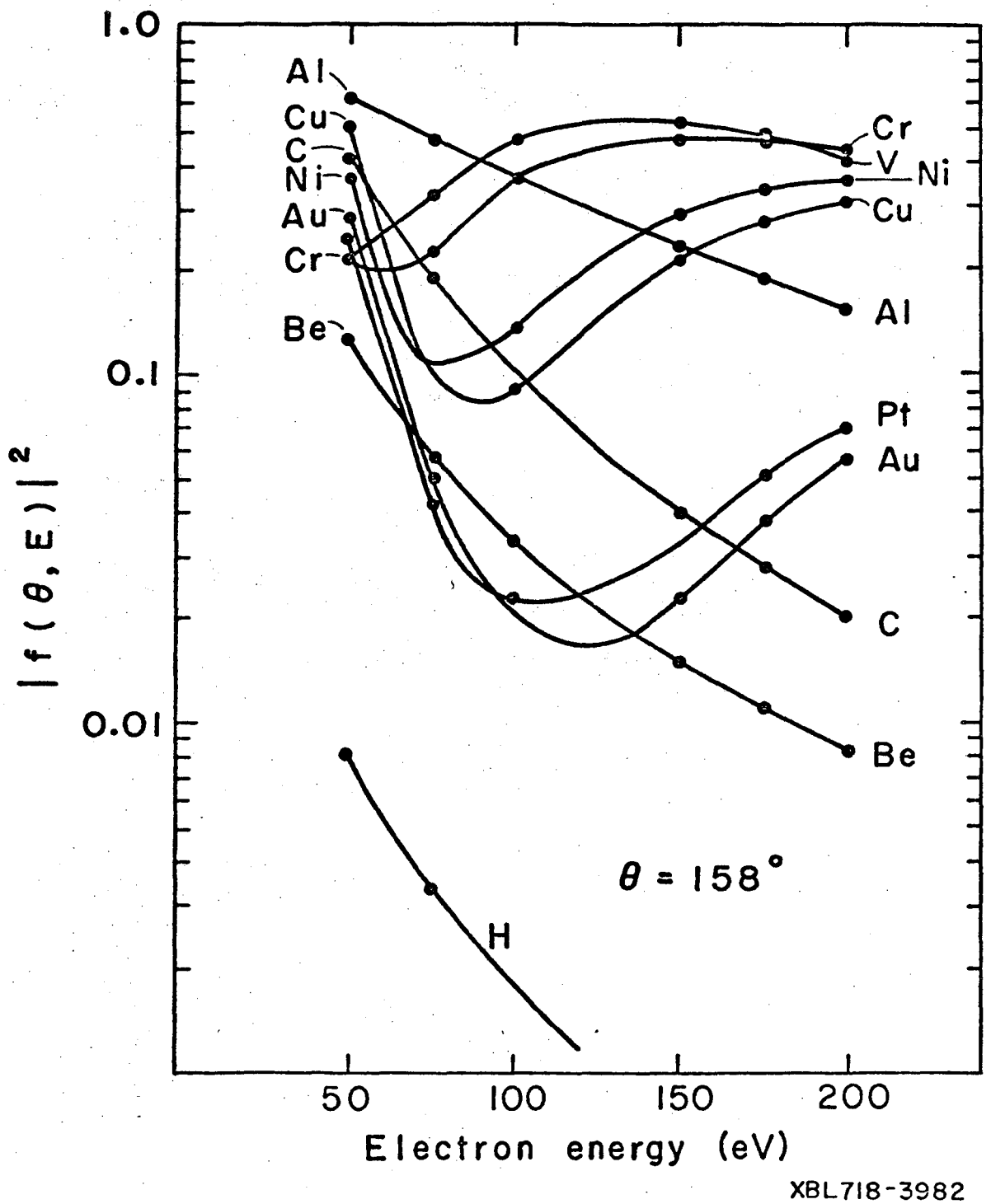
1.0
0.1
0.01
$|f(\theta,E)|^2$
Al
Cu
C
Ni
Au
Cr
Be
Cr
V
Ni
Cu
Al
Pt
Au
C
Be
H
$\theta = 158°$
50
100
150
200
Electron energy (eV)
XBL718-3982

Fig. 3

TECHNICAL INFORMATION DIVISION
LAWRENCE RADIATION LABORATORY
UNIVERSITY OF CALIFORNIA
BERKELEY, CALIFORNIA 94720

Presented at the Conference on High Voltage Electron Microscopy, Teddington, England, Sept. 22-23, 1971

LBL-145
Preprint c.1

AN ORTHOGONAL DRIVE TILTING STAGE FOR THE HITACHI 650 kV MICROSCOPE

James C. Hodges and Gareth Thomas

September 1971

AEC Contract No. W-7405-eng-48

LBL-145
c.1

DISCLAIMER

AN ORTHOGONAL DRIVE TILTING STAGE FOR THE HITACHI 650 kV MICROSCOPE

James C. Hodges* and Gareth Thomas†

Inorganic Materials Research Division, Lawrence Berkeley Laboratory
University of California, Berkeley, California

A specimen stage for the HU 650 Electron Microscope, giving up to ±14° tilt along two axes at 90°, is described. The development was prompted by metallurgical requirements for both greater range and more precise control of specimen tilting than available with the standard Hitachi tilt-rotation stage. The following design criteria were established:

1. The stage should be directly interchangeable with standard HU 650 stages, including hookup to existing drives entering the column wall.
2. There should be two separately controlled axes of tilt at 90°. These axes are to be oriented so as to parallel the translation axes of the microscope's built-in X-Y stage.
3. A tilt range of ±14° along each axis, if feasible within the standard immersion polepiece configuration, should be provided.
4. The intersection of the tilt axes should be fixed and centered at the specimen plane, so that a correspondingly centered specimen detail undergoes neither lateral nor vertical displacement during tilting.
4. The tilting actions are to respond smoothly and positively to manual fine-adjustment controls. Settings made with reference to tilt-angle indicators (graduated in either actual degrees or arbitrary units) must be accurately reproducible.

---

*Engineering Associate, Mechanical Technicians Department, Lawrence Berkeley Lab.
†Professor, Department of Materials Science and Engineering, College of Engineering, University of California, Berkeley.

In order to meet these requirements, several departures from conventional tilt-stage design were necessary. Push rods and opposing springs moving in guides normal to the beam axis could not be used; their lateral extensions to effect this amplitude of tilt would project well beyond the stage periphery. A conventional sphere-and-socket bearing at the specimen plane was ruled out due to its inability to prevent small rotational shifts of the specimen holder during tilting.

The push rod difficulty was solved by devising contoured push arms as shown in Figs. 1 and 2. Pivoted at their upper end, these arms extend downward along the tilt axes to contact the specimen cartridge sleeve where a small lateral movement effects the full range of tilt. Each push arm retracts into a cutout in the stage's sidewall to make room for the specimen cartrige as it approaches maximum closed-position tilt. Lever extensions with 45° offsets actuate the push arms. The offsets make it possible to align the tilt axes with the X-Y stage traverses, and the worm shafts with the existing imput shafts for the standard HU 650 stages.

Rotational or other instabilities at the specimen plane were avoided by fitting a full gimbal movement into this restricted space. Threaded pivots with locking setscrews are precisely adjustable to center the tilt axes' intersection and to take out all lateral or rotational play.

Additional features contributing to a positive, repeatable tilting action are:

1. Polished sapphire rods are set into the leading edges of the push arms. These serve both as straight-edge guides for the cartridge sleeve's orthogonal movements and as low friction cylindrical contacts for the vertical wiping action against the sleeve as an arm makes its tilting push.

2. The offset extension levers contact their actuating cams through ball-bearing rollers to minimize friction and wear.
3. The entire drive train of levers, cams and worm-sector gears is effectively preloaded against dead time or backlash by the pull of the spring attached to the cartridge sleeve.

As maximum tilts are made in sequence along each axis of an orthogonal tilting stage, the specimen cartridge rim traces the perimeter of a square. To avoid interference the stage must have a squared opening of equivalent size, or a circular opening which adequately circumscribes this square. In the present stage, the internal conical wall has been modified as an inverted quadrangular pyramid. The resulting squared faces obtain adequate clearance for the specimen cartridge to move through a full 30° of arc along either axis, even where a specimen tilt of up to plus/minus 15° has been preset for the other axis.

During these peripheral tilts, the electron beam traces a similar square on the upper face of the specimen cartridge. The size of this square is directly proportional to the maximum tilt angle (ϕ) and the height (h) of the cartridge above the tilt pivot at the specimen plane. (Side of square = $2 \tan\phi \times h$.) Since specimen cartridges cannot be precisely oriented during insertion (which is necessary if a square sperture is used), the minimum size opening to insure against beam occlusion at maximum tilts, will be the circumscribed circle to this calculated square. Unfortunately, this requirement cannot be met for the present stage, due to restrictions imposed by the HU 650's cartridge insertion and retrieval device. Each cartridge must be fitted with a transfer ring of fixed diameter which is positioned at a fixed minimal distance above the

specimen plane if the device is to grasp the cartridge for retrieval. This transfer ring restricts the cartridge's usable aperture to a circle considerably smaller than that required to circumscribe the square aperture needed for beam clearance at ±15° orthogonal tilts.

The relationship of usable (or optical) tilt to mechanical tilt range for the present stage can be visualized as a circle of ±14 units diameter centered in a square of ±15 units per side, as depicted in Fig. 3. It can be seen that large-angle tilts in all four quadrants are optically excluded. Also, when a near maximum 14° tilt has been preset on one axis, sweeps along the other axis are reduced to 1 or 2 degrees at most. Yet, mechanically, full ±15° sweeps can be made for any preset tilt of the other axis. Should these factors prove restrictive to information gathering from the specimen, modifications to the HU 650's cartridge handling device, enabling it to take a larger diameter transfer ring, are feasible.

Cam-actuated control of the push arms is a design feature of this stage intended to overcome a shortcoming of most orthogonal tilt stages--their inability to indicate actual degrees and direction of tilt. At present, contouring of the cams has been carried only to the extent needed to produce a reasonably linear ratio between increments of control shaft rotation and degrees of tilt. A backlash-free pulley and cable mechanism (interchangeable with the standard HU 650 stage drive) brings the two tilt controls from the specimen chamber down to the microscope's desk top. Pointers are geared to the multi-turn control knobs of this mechanism so that each pointer's sweep is less than 360° for full tilt range. A blank dial plate behind each pointer is then graduated mark by mark accoring to pointer position for optically verified degrees of tilt at the specimen.

Graduations obtained this way are good to perhaps ±1°. A fully corrected cam, however, would make possible the following refinements:

1. Multi-turn digital counters attached to the control drives and reading directly in tenths or hundredths-degree increments.
2. A means for accurately determining the azimuthal position of combined tilts, and of arbitrarily establishing new tilt axes. (An example of this is a simple belt tying the manual control knobs together. With corrected cams insuring simultaneous advances and/or retreats of the push arms, a new set of tilt axes would be generated at 45° to the original axes. As indicated in Fig. 3, tilts of up to ±21° can be obtained along these "diagonal" axes.)

Preliminary evaluations of this orthogonal tilting stage show that it functions well in high vacuum, and that the specimen can be tilted smoothly and reproducibly when observed at magnifications of 100,000×. Continuing use will determine actual need for refinements to optically utilize the full range of present mechanical tilts, or for installing fully corrected cams to gain added readout and off-axis tilt versatility. It is already evident that provisions for a high-temperature specimen heating unit or low temperature modifications would broaden the usefulness of this stage.

Acknowledgments

The authors are deeply grateful to the technicians, staff and graduate students for their advice and involvement in this project.

This work was done under the auspices of the U. S. Atomic Energy Commission through the Inorganic Materials Research Division of Lawrence Berkeley Laboratory.

Figure Captions

Fig. 1. Sectional view of the orthogonal tilting stage designed for the Hitachi HU 650 Electron Microscope. Push arms A, with sapphire rods B set into their leading edges, tilt and guide the specimen cartridge supporting sleeve C in two orthogonal directions. The lower neck of sleeve C forms part of a full gimbal with pivotal bearings located at the microscope's specimen plane. (See Fig. 2 for details of the actuating drive.)

Fig. 2. View from above of orthogonal tilting stage shown in Fig. 1. Imput from external control rotates shaft J and worm gear H. The mating sector worm wheel I moves through a small arc between limit stops. This movement is transferred via cam E, roller bearing F and offset extension arm D to the push arm A. Tension supplied by spring K holds cartridge C against the sapphire rod bearing and straight-edge B.

Fig. 3. Depicting tilt range limits at upper opening of specimen cartridge. Dots show electron beam position at various tilt extremes. Mechanical tilt range is shown by dashed square. Shaded areas are optically occluded by small diameter of transfer ring (heavy circle). Dashed circle is size of transfer ring which would permit full use of mechanical tilt.

Fig. 4. Side view of the orthogonal fitting stage with specimen holder inserted in the stage and tilted to the extreme X' position revealing the sapphire rod and push arm.

Fig. 5. Top view of the orthogonal fitting stage with specimen holder inserted in the stage.

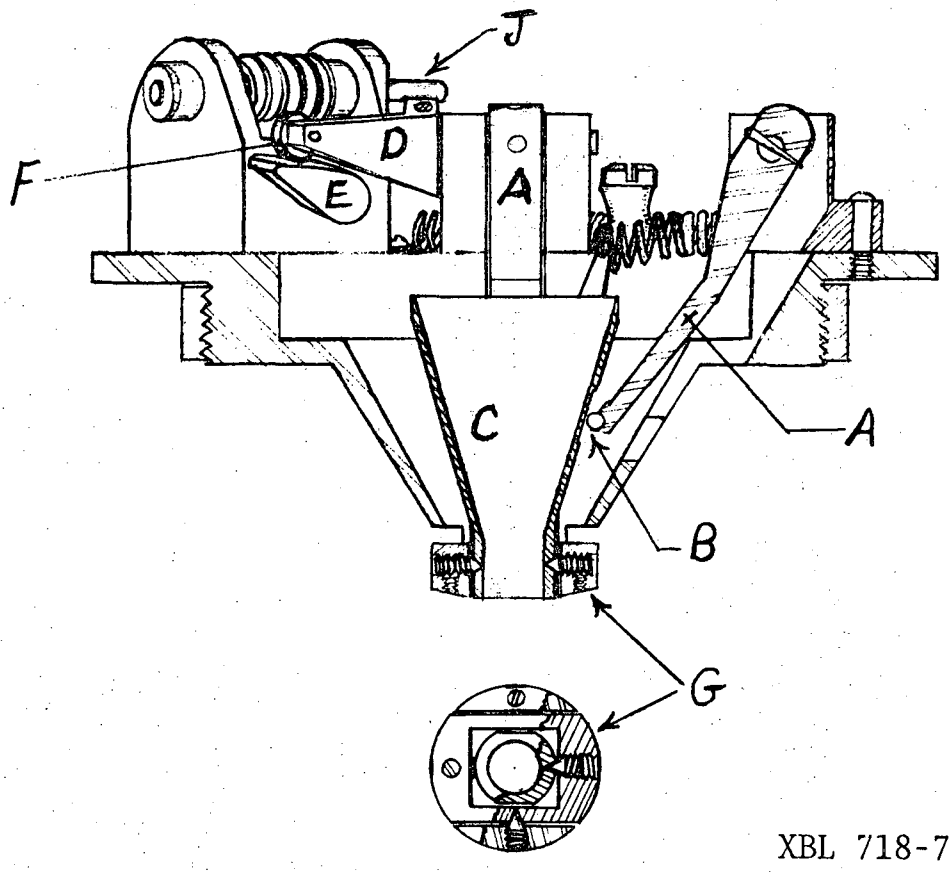

XBL 718-7122

Fig. 1

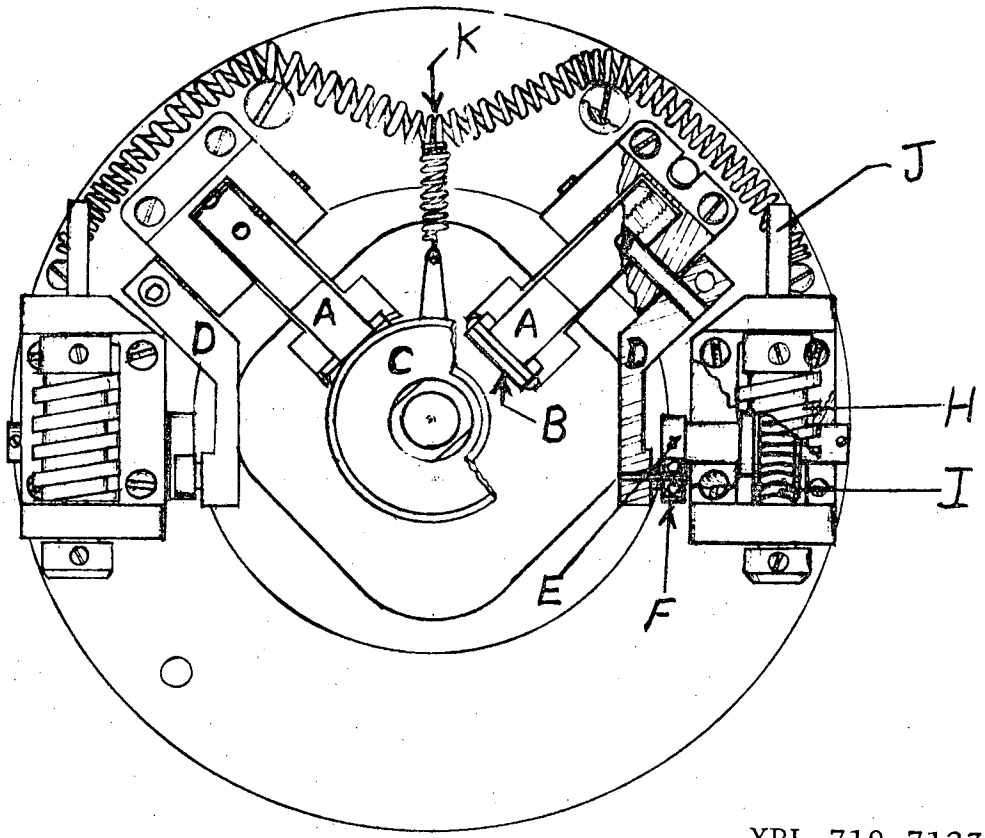

XBL 718-7123

Fig. 2

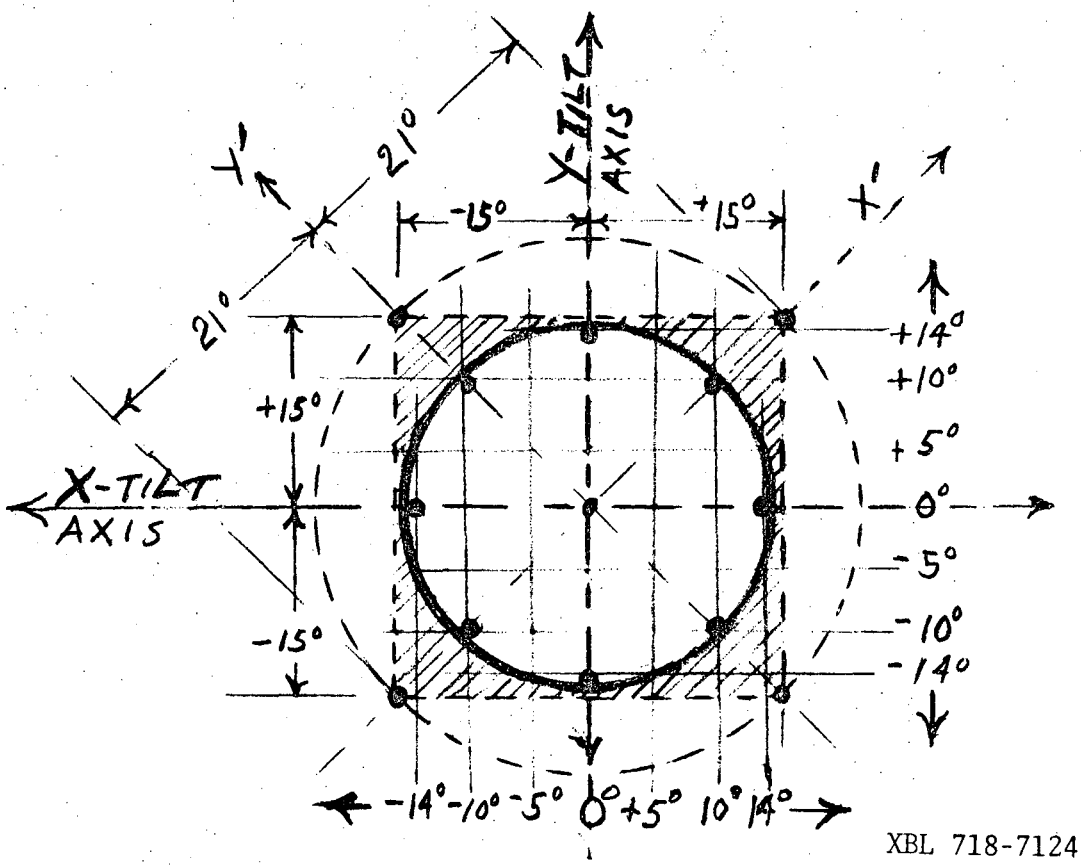
Y'
21°
21°
X-TILT AXIS
-15°
+15°
X'
+15°
-15°
X-TILT AXIS
+14°
+10°
+5°
0°
-5°
-10°
-14°
-14° -10° -5° 0° +5° 10° 14°
XBL 718-7124

Fig. 3

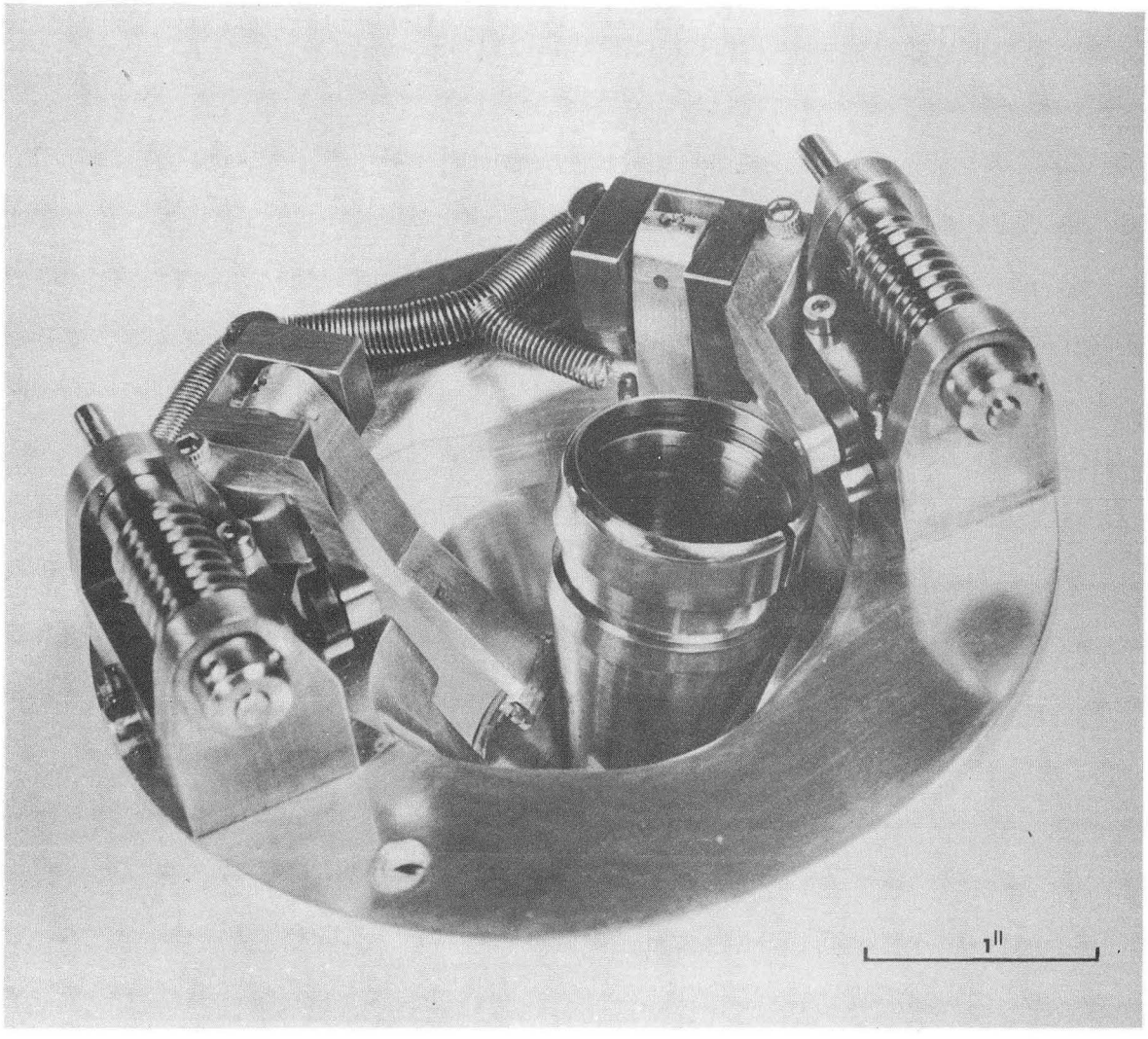

CBB 714-1422

Fig. 4

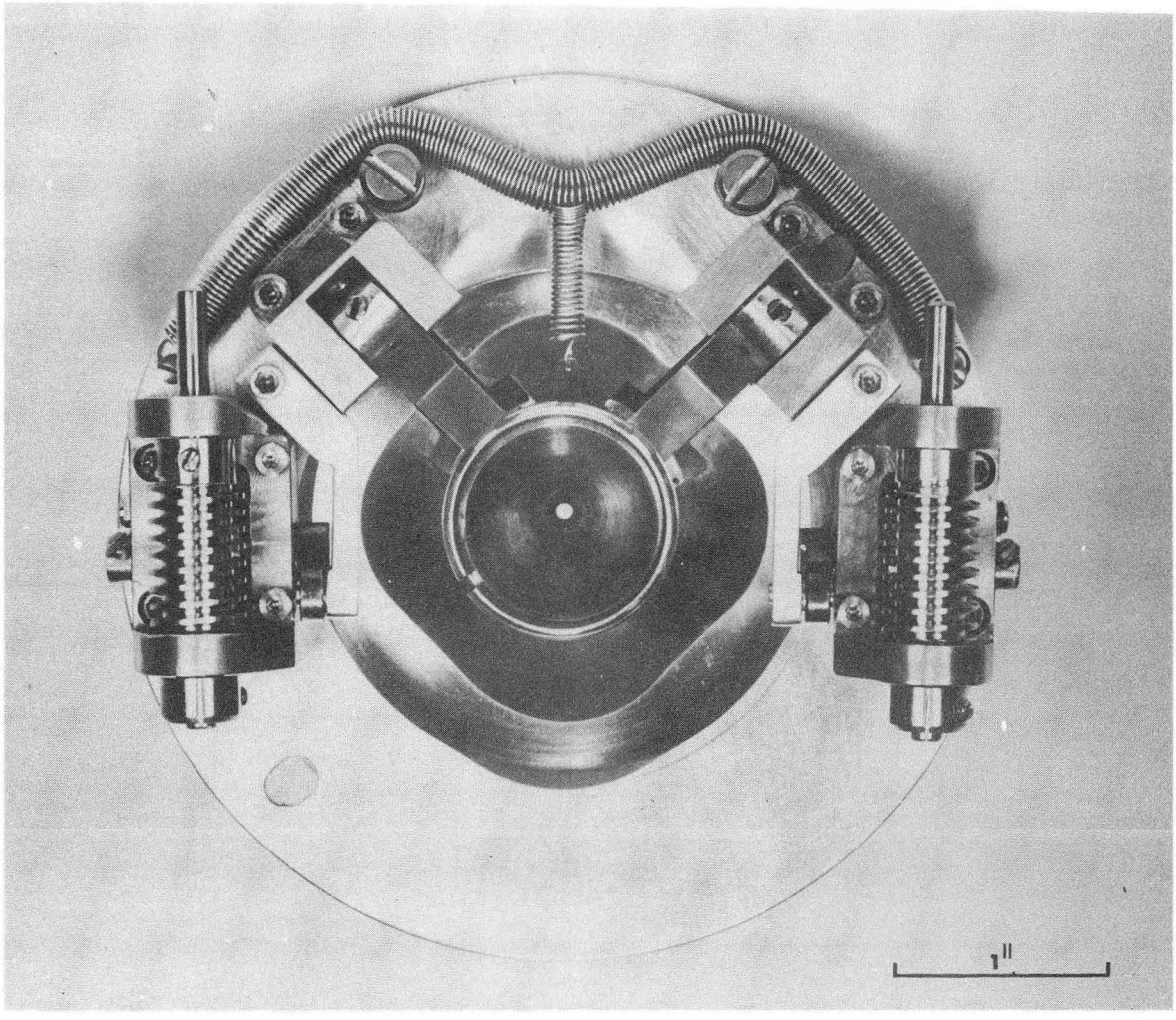

CBB 713-1124

Fig. 5

TECHNICAL INFORMATION DIVISION
LAWRENCE RADIATION LABORATORY
UNIVERSITY OF CALIFORNIA
BERKELEY, CALIFORNIA 94720